

# Physical Modeling of Hole Mobility in Silicon Inversion Layers under Uniaxial Stress

Ji Zhao, Jianping Zou, and Zhiping Yu

Institute of Microelectronics, Tsinghua University, Beijing, 100084, China

E-mail: zhaoji03@mails.tsinghua.edu.cn

## ABSTRACT

A physical model for hole mobility under both biaxial and uniaxial stress has been developed. The six-band  $k \cdot p$  theory is used to obtain the bandstructure with stress-dependent Hamiltonian. The hole mobility in the silicon inversion layer is studied in details using Monte Carlo method. A numerically robust method has been applied to achieve self-consistent solution of Poisson's and Schrödinger equations.

## INTRODUCTION

The uniaxial compressive stress has been used as an important technology for enhancing hole mobility. The theoretical models of hole mobility under biaxial stress have been studied [1,2]. Wang [3] has also discussed hole transport in inversion layers under arbitrary stress. This work is focused on hole mobility modeling under uniaxial stress of different orientation.

## BANDSTRUCTURE AND MOBILITY CALCULATIONS

We applied the six-band stress dependent  $k \cdot p$  theory to assemble the Hamiltonian in one-dimensional (1D) Schrödinger equation. We used self-consistent solution of Poisson's and Schrödinger equations to achieve the electronic structure in strained Si inversion layers. The self-consistency is achieved by applying a numerically efficient Newton-Broyden's method. The Monte Carlo procedure is used to evaluate the carrier transport under constant electric field and considering the scattering mechanisms of hole-phonon interaction, interface roughness, and Coulomb scattering.

## RESULTS AND DISCUSSION

First, we compare the convergence behavior of several different numerical, iterative methods in Fig. 1. It can be seen that the improved Newton-Broyden method has the best performance compared to the

standard Newton and standard Newton-Broyden methods. The calculated hole mobility vs. the effective electric field under unstrained Si, biaxial stress, and uniaxial stress are shown in Fig. 2 together with the experimental data for unstrained channel. Fig. 3 gives the first subband energy contours under unstrained and uniaxial compressive stress along the [110] direction with an effective field of 0.8MV/cm. Due to the effect of uniaxial stress the energy of regions K and L is lifted relative to the other regions M and N. More holes redistribute to the regions M and N with a low effective mass along the [110] direction. So, under uniaxial stress the mobility enhancement originates from an effective mass change and scattering suppression due to the splitting of band. The biaxial tensile stress, on the other hand, enhances mobility only through scattering suppression [3]. Fig. 4 shows the hole mobility under [110] and [100] uniaxial stress, respectively, and it is apparent that the hole mobility is larger in [110] than in [100] direction. Figs. 5-6 show the effective mass for the above two orientations and the mobility gain with the change in composition of Ge in SiGe.

## CONCLUSIONS

The effective mass and scattering suppression play the important roles in mobility enhancement. Uniaxial compressive stress along [110] direction enhances the hole mobility much more than in any other crystalline orientation. The physical model shows good agreement with experiment data.

## REFERENCES

- [1] M. Fischetti, *et al.*, "Six-band  $k \cdot p$  calculation of the hole mobility in silicon inversion layers: Dependence on surface orientation, strain, and silicon thickness," *J. Appl. Phys.* 94(2), 1079(2003)
- [2] R. Oberhuber, G. Zandler, and P. Vogl, "Subband structure and mobility of two-dimensional holes in strained Si/SiGe MOSFET's," *Phys. Rev. B*, 58(15), 9941(1998)
- [3] E. Wang, *et al.*, "Quantum mechanical calculation of hole mobility in silicon inversion layers under arbitrary stress," IEDM Digest, 2004

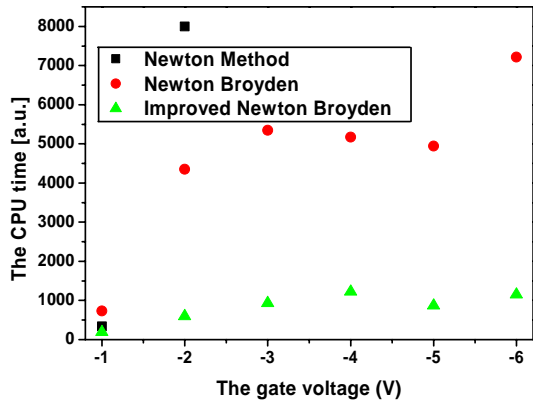


Fig. 1: The CPU time to achieve the consistent solution to 1D Schrödinger and Poisson's eqs. with various numerical method.

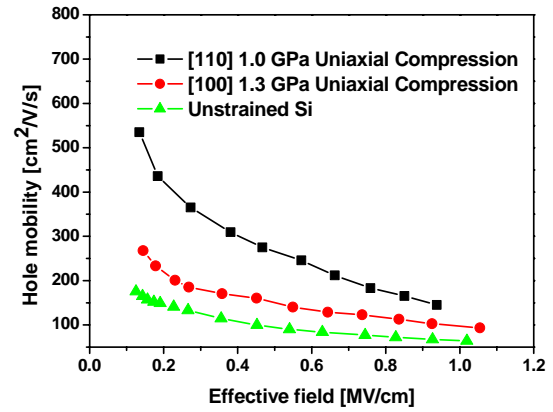


Fig. 4: The hole mobility in pMOS under unstrained and uniaxial compressive stress along the [110] and [100] direction, respectively, as a function of the effective electric field.

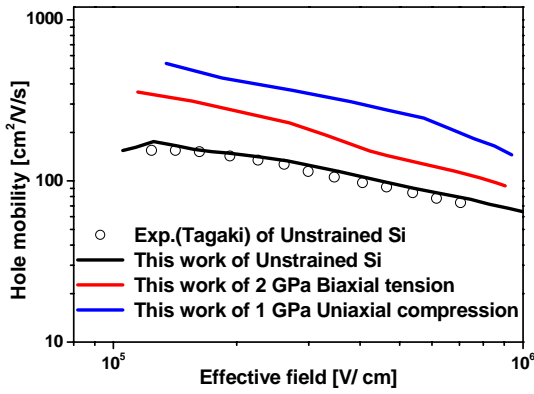


Fig. 2: Calculated hole mobility of pMOS under unstrained, biaxial tension and uniaxial compression as a function of the effective electric field.

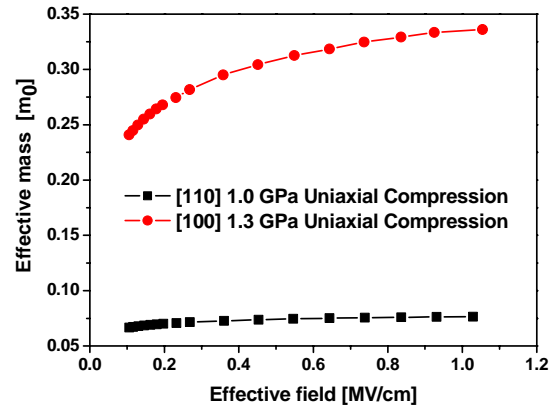


Fig. 5: The first subband hole effective mass of pMOS under uniaxial compressive stress along the [110] and [100] direction as a function of the effective electric field.

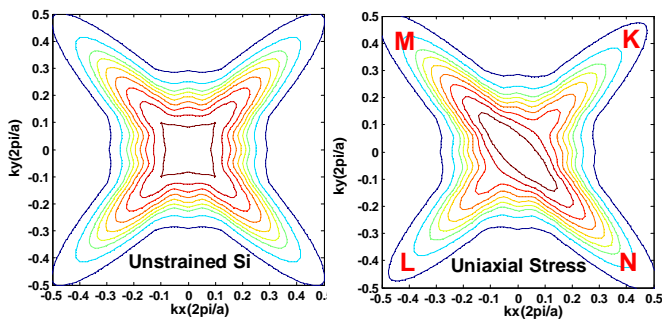


Fig. 3: First subband energy contours for valence band with an effective field of 0.8  $\text{MV/cm}$  under no stress and 1 GPa uniaxial compressive stress along [110].

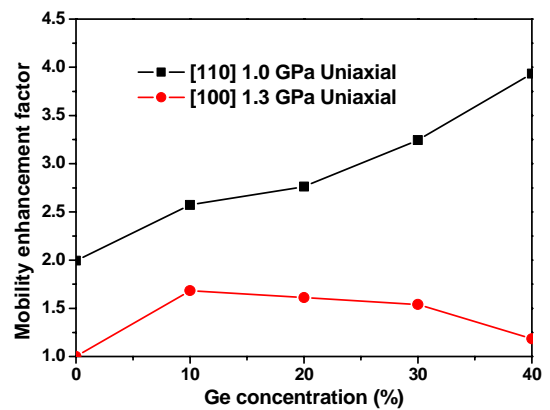


Fig. 6: The hole mobility enhancement factor of pMOS under uniaxial compressive stress along the [110] and [100] direction as a function of the Ge mole fraction in SiGe.